

# Обзор ArXiv/astro-ph 14-19 октября 2023

От Сильченко О.К.

# ArXiv: 2310.11493

## $\Sigma_{\text{SFR}}-M_*$ Diagram: A Valuable Galaxy Evolution Diagnostic to Complement (s)SFR- $M_*$ Diagrams

Samir Salim<sup>1</sup>, Sandro Tacchella<sup>2,3</sup>, Chandler Osborne<sup>1</sup>, S. M. Faber<sup>4</sup>, Janice C. Lee<sup>5</sup>, and Sara L. Ellison<sup>6</sup>

<sup>1</sup>*Department of Astronomy, Indiana University, Bloomington, IN 47405, USA*

<sup>2</sup>*Kavli Institute for Cosmology, University of Cambridge, Madingley Road, Cambridge, CB3 0HA, UK*

<sup>3</sup>*Cavendish Laboratory, University of Cambridge, 19 JJ Thomson Avenue, Cambridge, CB3 0HE, UK*

<sup>4</sup>*Department of Astronomy and Astrophysics, University of California, Santa Cruz, CA, 95064, USA*

<sup>5</sup>*Space Telescope Science Institute, Baltimore, MD, 21218, USA*

<sup>6</sup>*Department of Physics & Astronomy, University of Victoria, Victoria, British Columbia, V8P 1A1, Canada*

### Abstract

The specific star formation rate (sSFR) is commonly used to describe the level of galaxy star formation (SF) and to select quenched galaxies. However, being a relative measure of the young-to-old population, an ambiguity in its interpretation may arise because a small sSFR can be either because of a substantial previous mass build up, or because SF is low. We show, using large samples spanning  $0 < z < 2$ , that the normalization of SFR by the physical extent over which SF is taking place (i.e., SFR surface density,  $\Sigma_{\text{SFR}}$ ) overcomes this ambiguity.  $\Sigma_{\text{SFR}}$  has a strong physical basis, being tied to the molecular gas density and the effectiveness of stellar feedback, so we propose  $\Sigma_{\text{SFR}}-M_*$  as an important galaxy evolution diagram to complement (s)SFR- $M_*$  diagrams. Using the  $\Sigma_{\text{SFR}}-M_*$  diagram we confirm the Schiminovich et al. (2007) result that the level of SF along the main sequence today is only weakly mass dependent—high-mass galaxies, despite their redder colors, are as active as blue, low-mass ones. At higher redshift, the slope of the “ $\Sigma_{\text{SFR}}$  main sequence” steepens, signaling the epoch of bulge build-up in massive galaxies. We also find that  $\Sigma_{\text{SFR}}$  based on the optical isophotal radius more cleanly selects both the starbursting and the spheroid-dominated (early-type) galaxies than sSFR. One implication of our analysis is that the assessment of the inside-out vs. outside-in quenching scenarios should consider both sSFR and  $\Sigma_{\text{SFR}}$  radial profiles, because ample SF may be present in bulges with low sSFR (red color).

# Классики хотят определений:

Before proceeding, it is worthwhile to discuss the definition of the verb ‘quenching’ and adjective ‘quenched’, since we will often refer to them. As pointed out by Belfiore et al. (2018), Donnari et al. (2019) and others, there is no agreed upon definition of the verb ‘quenching’. Definition of quenching is relatively unambiguous for individual SF histories, especially the idealized ones. For them, the quenching represents a downward change in SFR with respect to some gradual overall trend. For example, Martin et al. (2007), one of the first studies on quenching, defines it as an exponential decline with a variety of quenching rates ( $e$ -folding times 0.5 to 20 Gyr) following a *constant* SFR. Given the difficulties in constraining the SF histories of individual galaxies, and the fact that their forms in reality contain complex details (Pandya et al. 2017), a definition that is based on the properties of an ensemble of galaxies would be more useful. Thus, the definition that Belfiore et al. (2018) and many other studies use, and the one we will for most part use here, is that ‘quenching’ refers to a *process that moves the galaxies below the main sequence*. For a galaxy of a certain mass, being below the main sequence implies a different SF history than of other galaxies of the same mass—one that currently has a lower SFR.

Using an adjective ‘quenched’ to define a galaxy with *no* SF, can be considered an *absolute* definition. Note that one can alternatively consider a galaxy as quenched when its SFR no longer contributes to the build-up of a galaxy on some relevant timescales, such as the Hubble time at the epoch of observation. Such *relative* definition is closely tied to the sSFR (Tacchella et al. 2018), since the inverse of sSFR represents the time needed to double the stellar mass (modulo gas recycling). A galaxy with  $\log \text{sSFR} = -10.1$  today will take a Hubble time to double its mass, so one can think of it as having finished most of its assembly and thus in a certain way quenched. If one uses this relative definition of being quenched, then sSFR is, by definition, the only way to identify quenched galaxies. In this paper, we will assume the

## Absolute definition

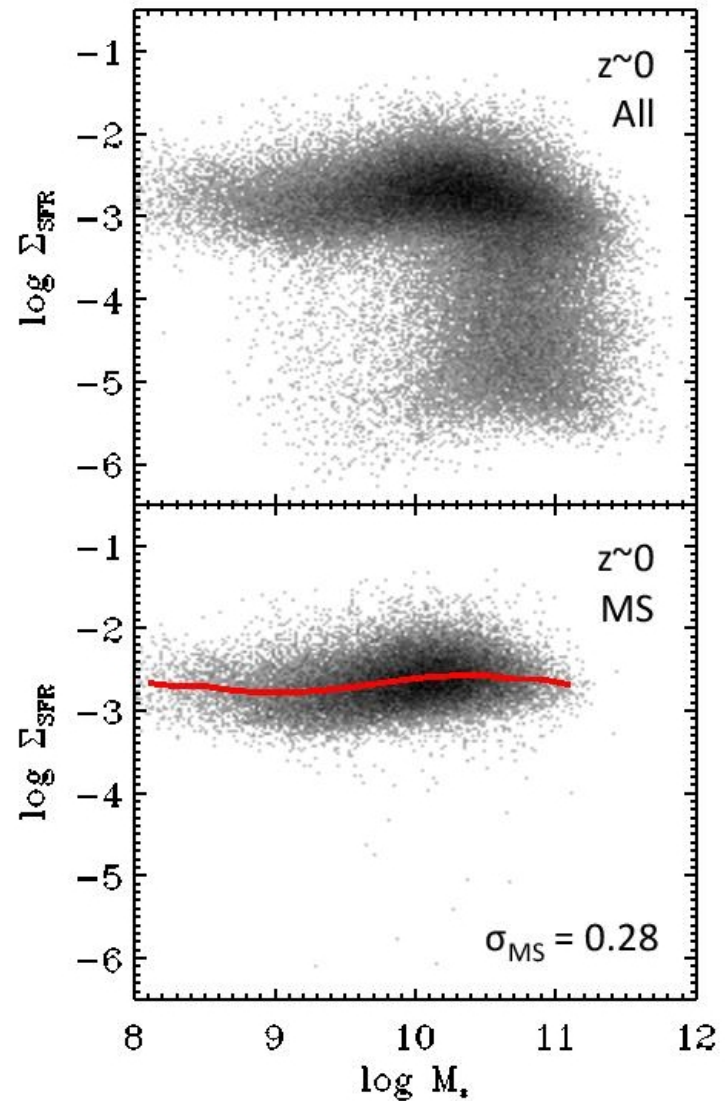
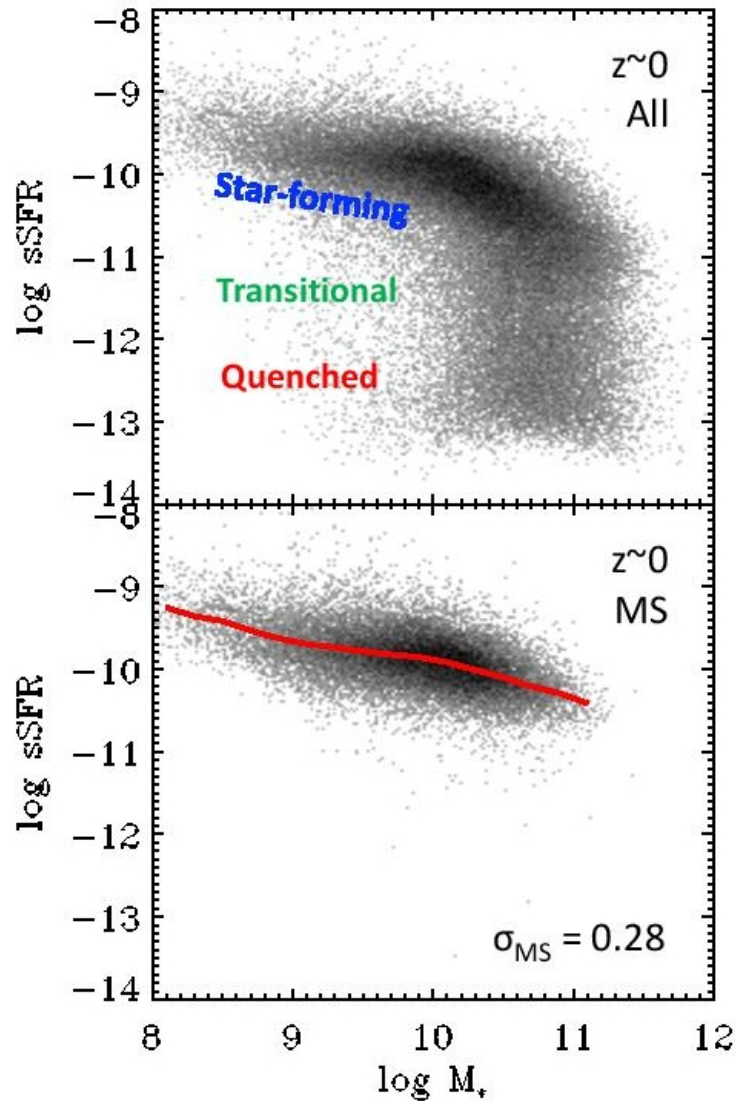
# Samples:

- Z=0: Salim+2016 GSWLC-2: 175k  $\rightarrow$  77k  $\rightarrow$  29k (emission) (4000 Abraham & Naim' morphology, 639 mergers, Darg 2010);
- Z=1: CANDELS 1905 galaxies
- Z=2: CANDELS 1550 galaxies

Изофотный радиус: 25я в r (H if z=1 or z=2)



# Главная последовательность



# Вспышечное звездообразование (mergers)

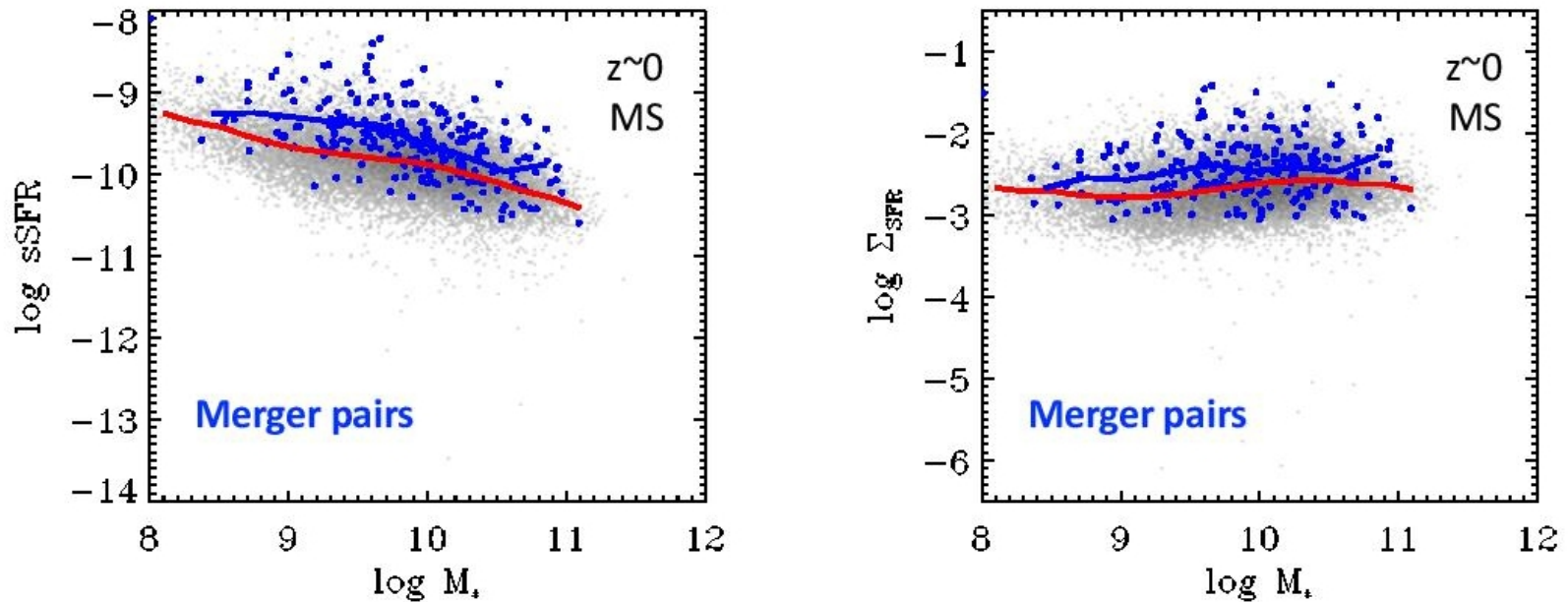
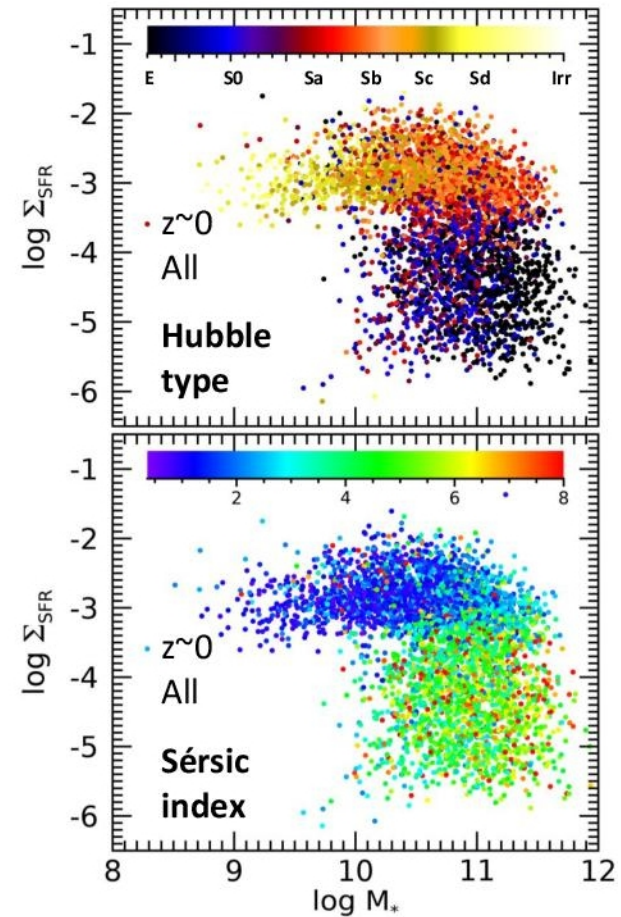
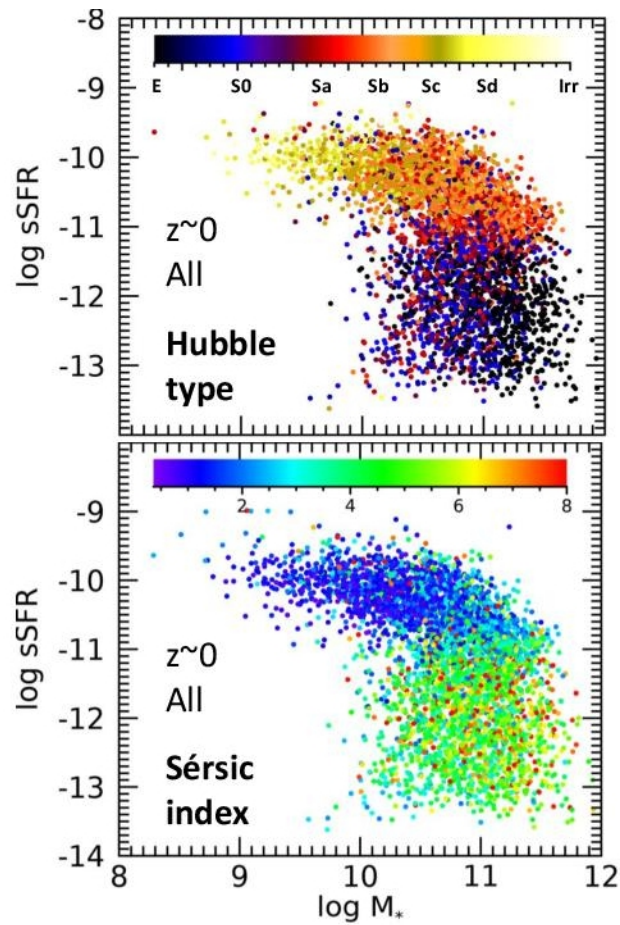


**Figure 3.** Main-sequence merger pairs (interacting galaxies) over-plotted on the general low-redshift main sequence population. Same galaxies are shown on the  $\text{sSFR}-M_*$  (left) and  $\Sigma_{\text{SFR}}-M_*$  diagrams (right). Merger pairs serve as proxies for starbursts and come from Darg et al. (2010). Merging galaxies have a similar average offset (blue line) from the ridge of the overall main sequence (red line) in both cases; however, because there is no mass dependence, selecting starbursts by SFR surface density is obviously much cleaner than based on sSFR.

# «Зеленая долина»



# Большие красные смещения

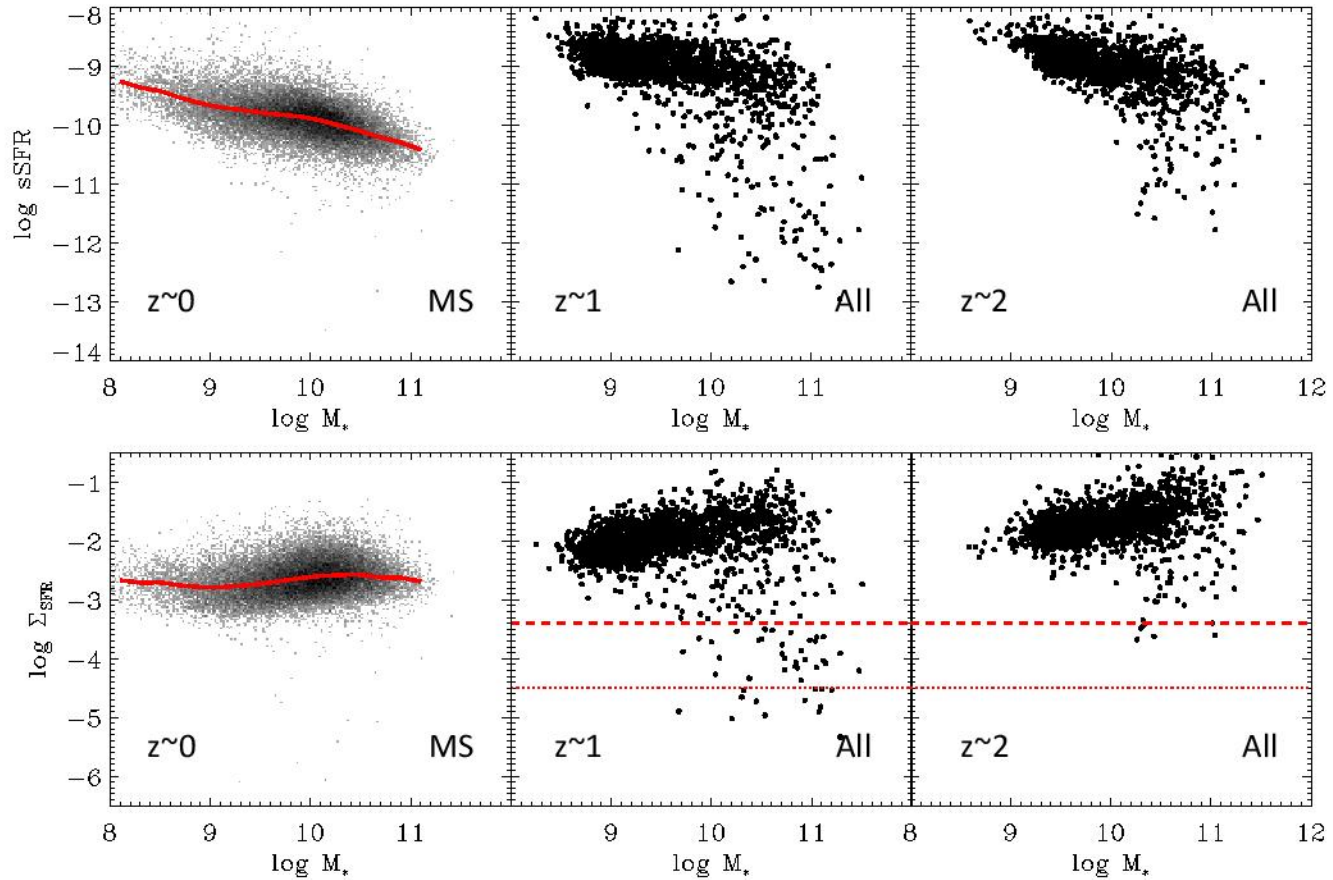
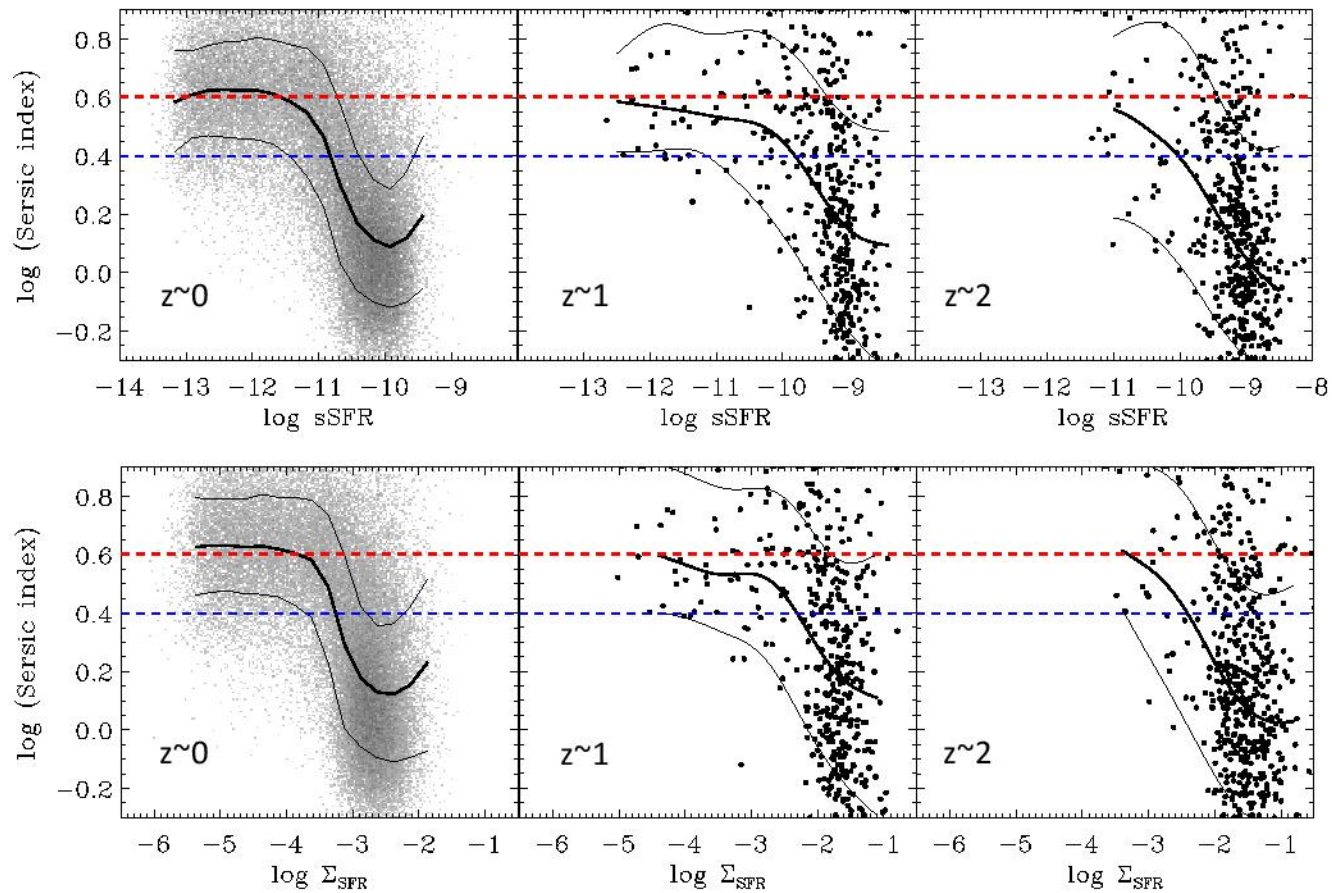


Figure 5 Evolution of stellar mass ( $M_*$ ) and  $\Sigma_{sSFR}$  vs  $M_*$  (dotted line) and  $\Sigma_{sSFR}$  vs  $M_*$  (dashed line) Evolution of the star formation rate (sSFR) vs stellar mass ( $M_*$ ) and  $\Sigma_{sSFR}$  vs  $M_*$  (dotted line) Evolution of the star formation rate surface density ( $\Sigma_{sSFR}$ ) vs stellar mass ( $M_*$ ) and  $\Sigma_{sSFR}$  vs  $M_*$  (dashed line)



# На больших $z$ звздообразование захватывает балджи



# Пора отказываться от red sequence/blue cloud по цвету!

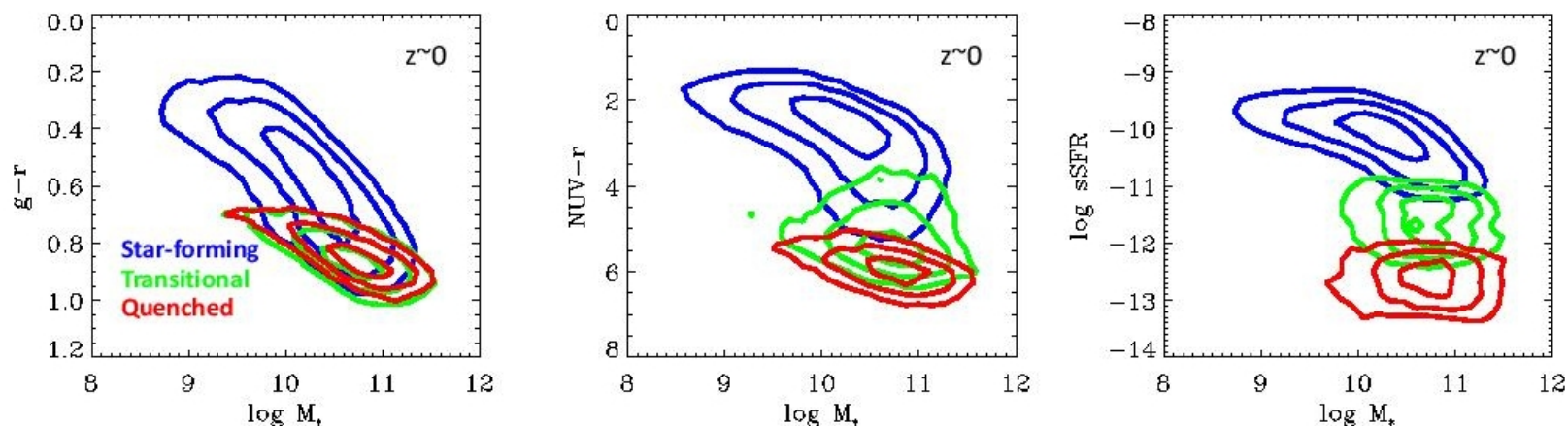


**Figure 8.** The placement of galaxies separated into star-forming, transitional and quenched (quiescent) categories on various diagrams with stellar mass on the  $x$  axis. Panels from left to right demonstrate the successive improvements in the ability to separate these categories afforded by moving from optical to UV-optical color and then to sSFR. Specific SFRs provide a good separation between these categories, but the use of  $\Sigma_{SFR}$  (based on which these categories have been defined) goes an additional step by eliminating the effect of age on the main sequence (its tilt).

# ArXiv: 2310.11872

## MUSE observations of the giant low surface brightness galaxy Malin 1: Numerous HII regions, star formation rate, metallicity, and dust attenuation

Junais<sup>1</sup>, P. M. Weilbacher<sup>2</sup>, B. Epinat<sup>3,4</sup>, S. Boissier<sup>3</sup>, G. Galaz<sup>5</sup>, E. J. Johnston<sup>6</sup>, T. H. Puzia<sup>5</sup>, P. Amram<sup>2</sup>, K. Małek<sup>1,2</sup>

<sup>1</sup> National Centre for Nuclear Research, Pasteura 7, PL-02-093 Warsaw, Poland  
e-mail: junais@ncbj.gov.pl

<sup>2</sup> Leibniz-Institut für Astrophysik Potsdam (AIP), An der Sternwarte 16, 14482 Potsdam

<sup>3</sup> Aix Marseille Univ, CNRS, CNES, LAM, Marseille, France

<sup>4</sup> Canada-France-Hawaii Telescope, 65-1238 Mamalahoa Highway, Kamuela, HI 96743, USA

<sup>5</sup> Instituto de Astrofísica, Pontificia Universidad Católica de Chile, Avenida Vicuña Mackenna 4860, 7820436 Macul, Santiago, Chile

<sup>6</sup> Instituto de Estudios Astrofísicos, Facultad de Ingeniería y Ciencias, Universidad Diego Portales, Av. Ejército Libertador 441, Santiago, Chile

Received 07 August 2023/ Accepted 18 October 2023

### ABSTRACT

*Context.* Giant low-surface brightness (GLSB) galaxies are an extreme class of objects with very faint and extended gas-rich disks. Malin 1 is the largest GLSB galaxy known to date, and one of the largest individual spiral galaxies observed so far, but the properties and formation mechanisms of its giant disk are still poorly understood.

*Aims.* We use VLT/MUSE IFU spectroscopic observations of Malin 1 to measure the star formation rate, dust attenuation, and gas metallicity within this intriguing galaxy.

*Methods.* We performed a pPXF modeling to extract emission line fluxes such as  $H\alpha$ ,  $H\beta$ ,  $[N\ II]_{6583}$  and  $[O\ III]_{5007}$  along the central region as well as the extended disk of Malin 1.

*Results.* Our observations reveal, for the first time, the presence of strong  $H\alpha$  emission distributed across numerous regions along the extended disk of Malin 1, reaching up to radial distances of  $\sim 100$  kpc, indicating recent star formation activity. We made an estimate of the dust attenuation in the disk of Malin 1 using the Balmer decrement and found that Malin 1 has a mean  $H\alpha$  attenuation of 0.36 mag. We observe a steep decline in the radial distribution of star formation rate surface density ( $\Sigma_{SFR}$ ) within the inner 20 kpc, followed by a shallow decline in the extended disk. We estimated the gas phase metallicity in Malin 1, and also found for the first time, that the metallicity shows a steep gradient in the inner 20 kpc of the galaxy from solar metallicity to sub-solar values, followed

# Malin 1

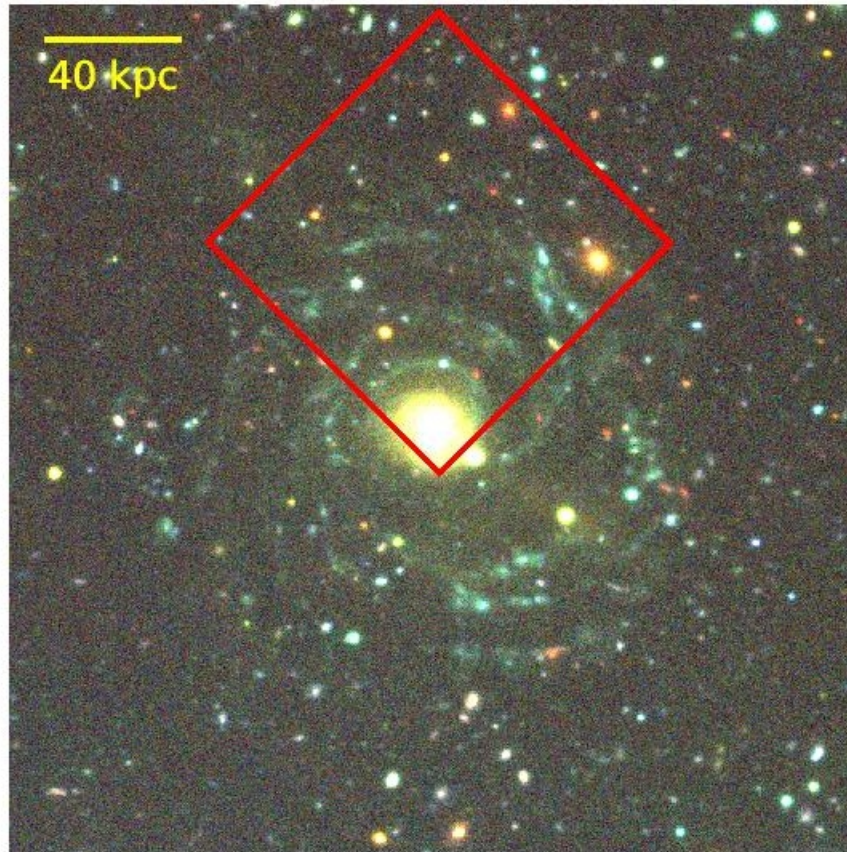


Fig. 1: Colour composite image of Malin 1 from the CFHT-Megacam NGVS (Ferrarese et al. 2012)  $u$ ,  $g$ , and  $i$ -band images.



# Эмиссионные линии в Malin1

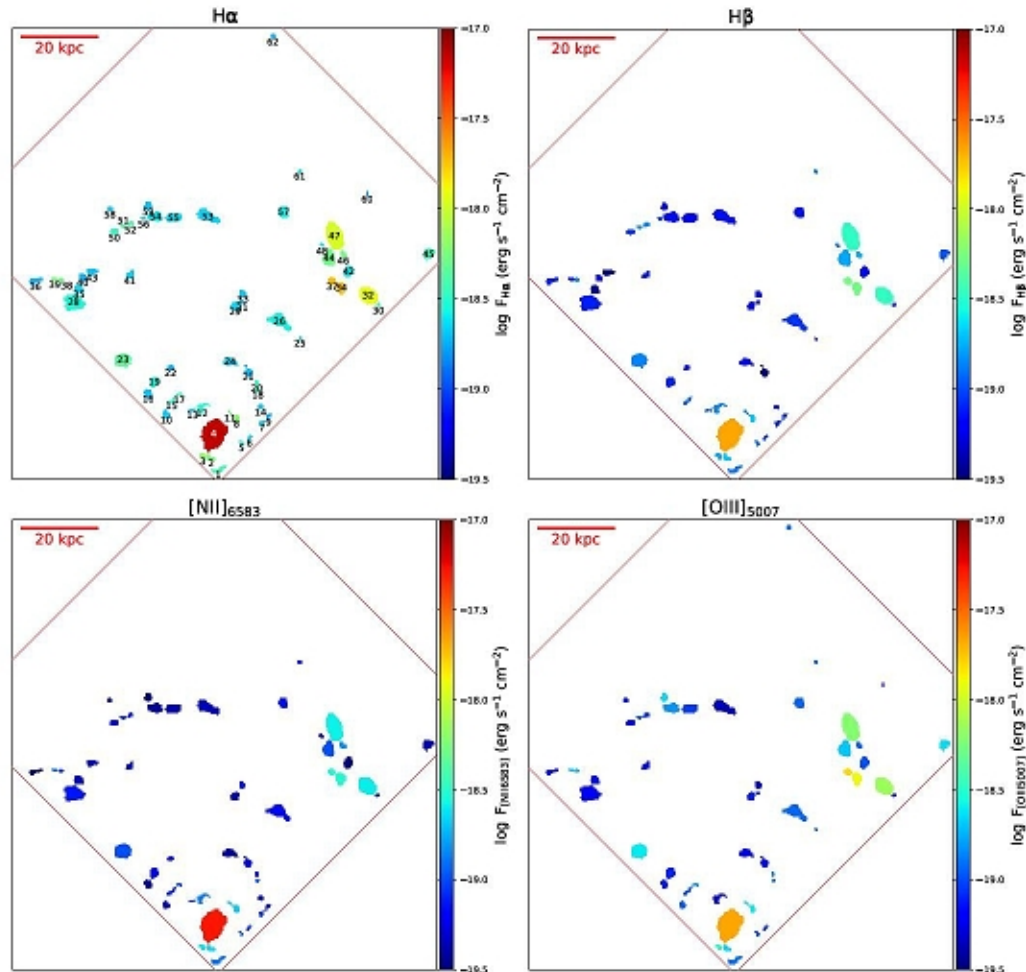


Fig. 3: Emission line flux maps of Malin 1 obtained from the pPXF fitting of the HII regions. The  $H\alpha$ , and the  $H\beta$  lines are in the top panels, whereas the  $[N II]_{6583}$  and the  $[O III]_{5007}$  lines are along the bottom panels. The ID of each region, as discussed in Sect. 2.2.2, is labeled in black in the top left panel. The regions with ID 27 and 49 are excluded from the maps as they do not have an SNR > 2.5 in any of the emission lines. The color bar indicates the flux corresponding to each emission line. Note that the flux value of each region is given as the average flux per pixel within that region obtained from the fitting of its row-stacked spectrum.

# Поглощение

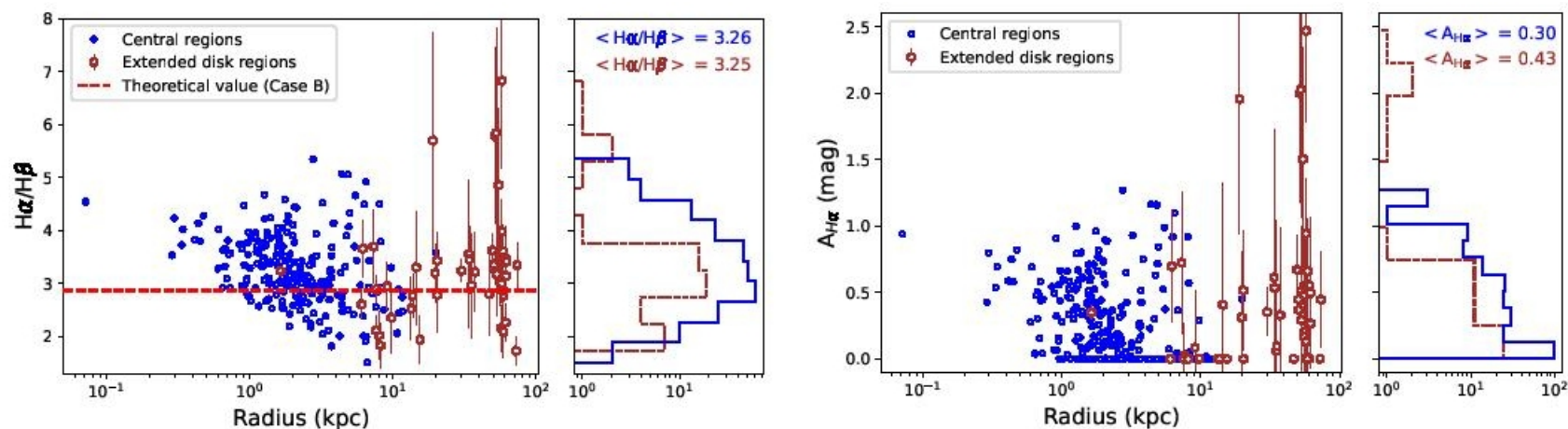


Fig. 4: Radial variation of Balmer ratio (left panel) and  $H\alpha$  attenuation (right panel). The blue circles and the brown hexagons are the central regions and the extended disk regions, respectively, obtained from the pPXF fit discussed in Sect. 2.2. The red horizontal dashed line marks the intrinsic Balmer ratio of 2.86 for Case B recombination. To all regions with the Balmer ratio below this value, we assign zero attenuation. The histograms beside each panel give the overall distribution of each quantity (blue solid line and brown dashed line for the central region and extended disk, respectively), with their mean values indicated at the top of each panel.

# Темпы звездообразования

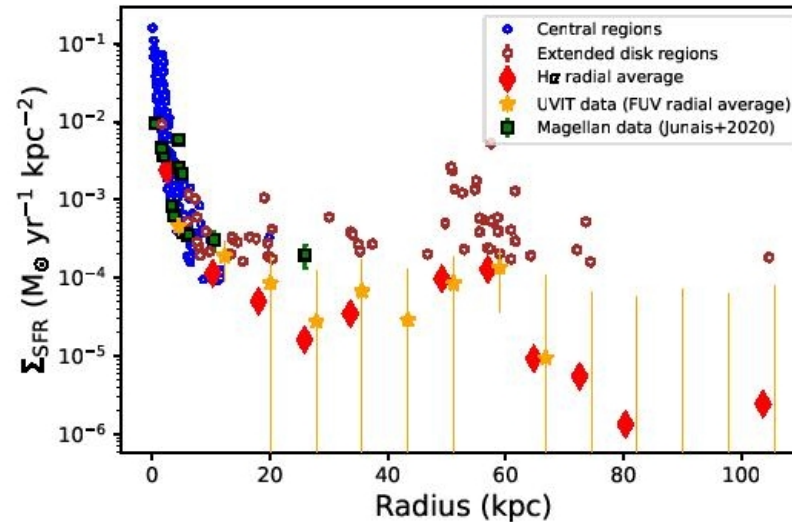


Fig. 5: Star formation rate surface density of Malin 1 as a function of galactocentric radius. The blue circles and the brown hexagons are the central regions and the extended disk regions, respectively, obtained from the pPXF fit discussed in Sect. 2.2. The red diamonds are the  $H\alpha$  radial average measured along concentric rings of  $5''$  width from the center. The orange stars are the radial averages measured on the same field in the UVIT FUV image of Malin 1 from Saha et al. (2021), as shown in Fig. 6. For illustration purposes, the UV data points are horizontally shifted by 2 kpc. The green squares are the data points from Junais et al. (2020), based on the IMACS-Magellan  $H\alpha$  long-slit spectra of Malin 1.

# Ультрафиолет

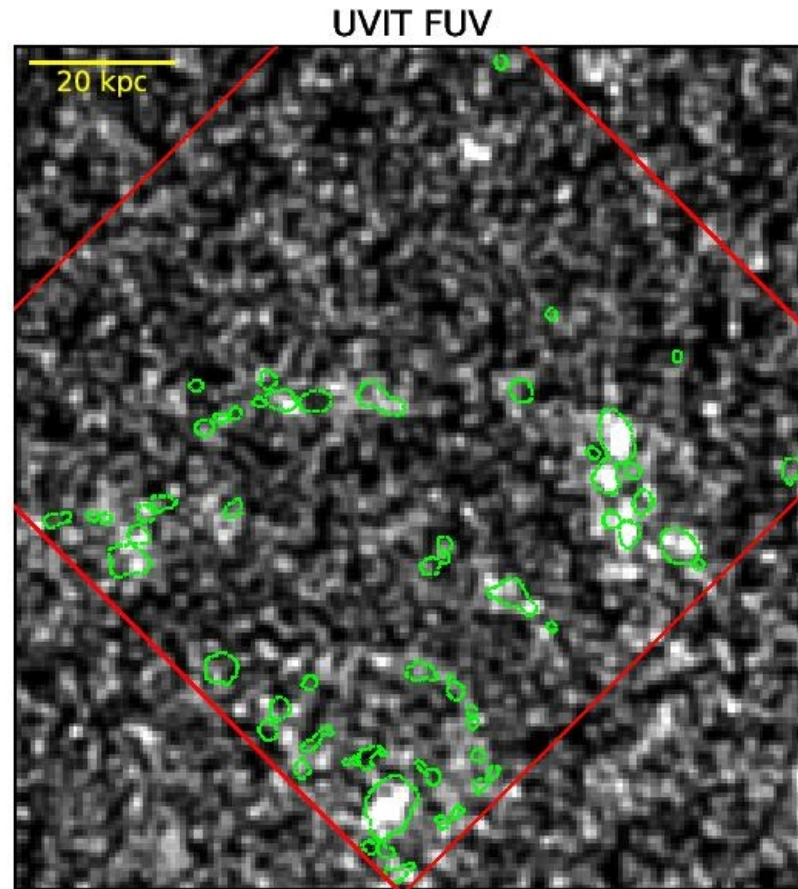


Fig. 6: FUV image of Malin 1 from [Saha et al. \(2021\)](#) of the same field as our MUSE observations (shown as the red box). The green contours mark the  $H\alpha$ -detected regions as discussed in Sect. [2.2.2](#).



# Металличность

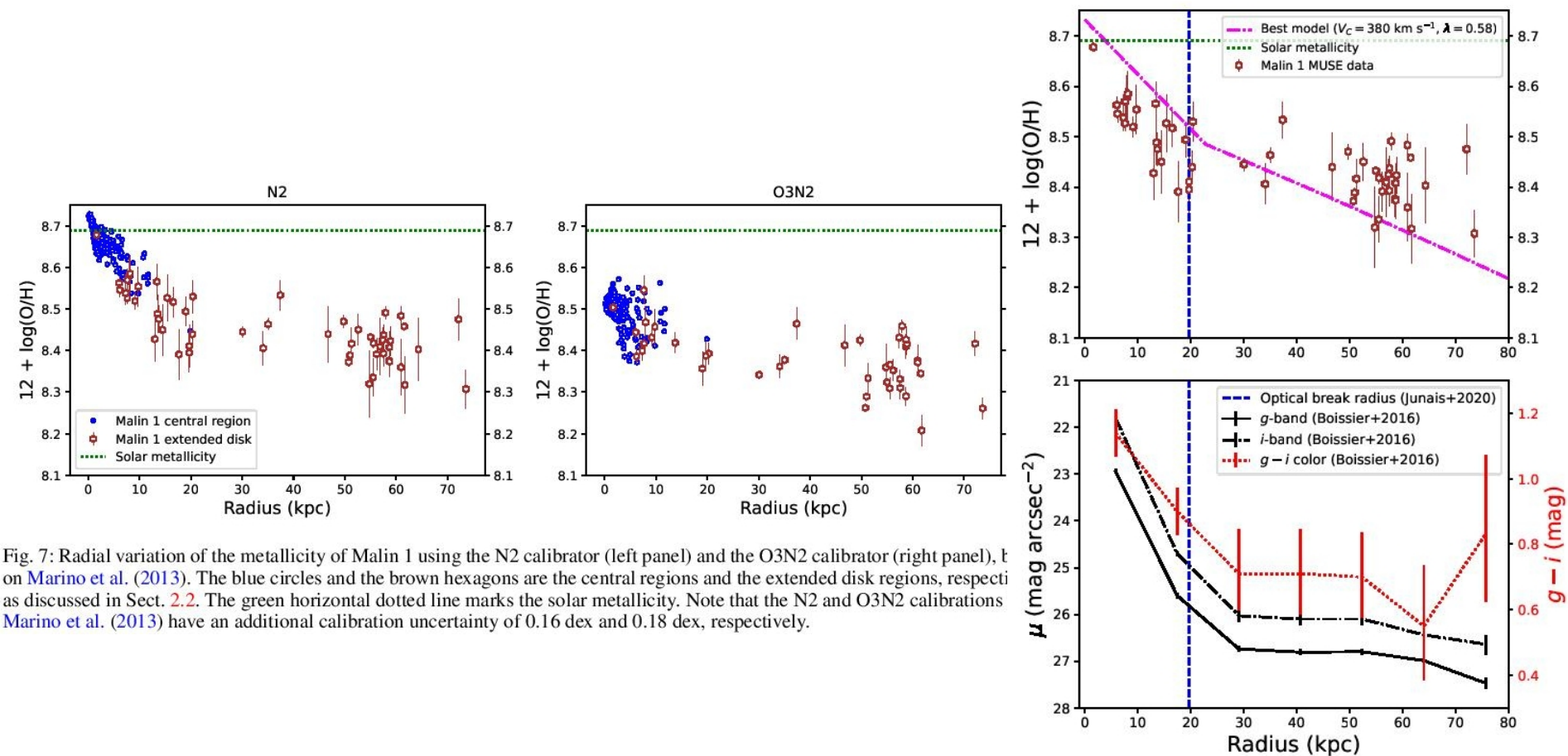


Fig. 7: Radial variation of the metallicity of Malin 1 using the N2 calibrator (left panel) and the O3N2 calibrator (right panel), taken from Marino et al. (2013). The blue circles and the brown hexagons are the central regions and the extended disk regions, respectively, as discussed in Sect. 2.2. The green horizontal dotted line marks the solar metallicity. Note that the N2 and O3N2 calibrations from Marino et al. (2013) have an additional calibration uncertainty of 0.16 dex and 0.18 dex, respectively.

# Эффективность звездообразования — ниже средней

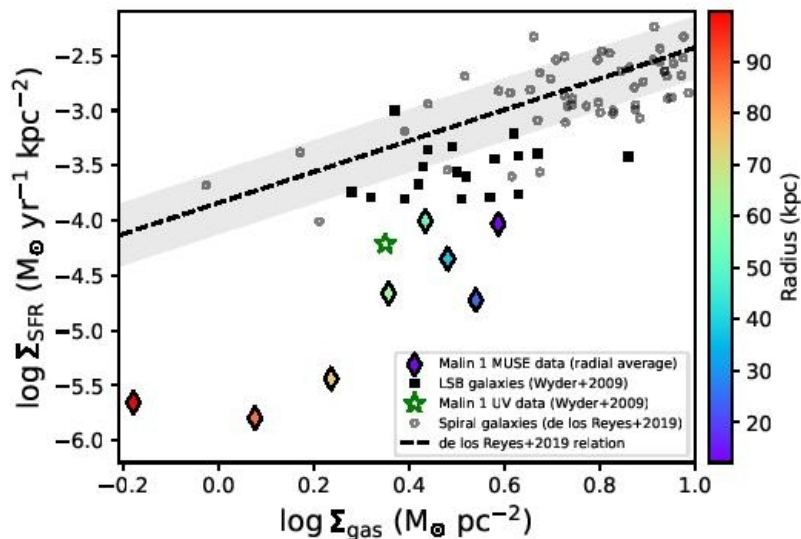


Fig. 9: Star formation rate surface density versus gas surface density. The diamond symbols mark the region along the disk of Malin 1 based on the radial averaged  $\Sigma_{\text{SFR}}$  we estimated as in Fig. 5. The  $\Sigma_{\text{gas}}$  for Malin 1 is from the eight H I data points of Lelli et al. (2010), after correcting for the Helium by a factor of 1.4. The color bar indicates the radius along the disk of Malin 1. The black open circles are normal spiral galaxies from de los Reyes & Kennicutt 2019 (the  $\Sigma_{\text{gas}}$  from de los Reyes & Kennicutt 2019 uses the total atomic and molecular gas mass). The black dashed line and the grey shaded region are the de los Reyes & Kennicutt (2019) best-fit relation and  $1\sigma$  scatter. The black squares are the LSB galaxies from Wyder et al. (2009), along the Malin 1 marked as the open green star symbol based on the UVF estimation from Wyder et al. (2009).